J.W. Hightower, W.N. Delgass, E. Iglesia and A.T. Bell (Eds.)
11th International Congress on Catalysis - 40th Anniversary
Studies in Surface Science and Catalysis, Vol. 101

Design of stable catalysts for methane-carbon dioxide reforming

J.A. Lercher, J.H. Bitter, W. Hally, W. Niessen, and K. Seshan

Faculty of Chemical Technology, Catalytic Processes and Materials Group,
University of Twente, P.O. Box 217, 7500 AE, Enschede, The Netherlands

Abstract

The activity and stability of catalysts for methane-carbon dioxide reforming depend subtly upon the support and the active metal. Methane decomposes to carbon and hydrogen, forming carbon on the oxide support and the metal. Carbon on the metal is reactive and can be oxidized to CO by oxygen from dissociatively adsorbed CO_2. For noble metals this reaction is fast, leading to low coke accumulation on the metal particles. The rate of carbon formation on the support is proportional to the concentration of Lewis acid sites. This carbon is non reactive and may cover the Pt particles causing catalyst deactivation. Hence, the combination of Pt with a support low in acid sites, such as ZrO_2 is well suited for long term stable operation. For non-noble metals such as Ni, the rate of CH_4 dissociation exceeds the rate of oxidation drastically and carbon forms rapidly on the metal in the form of filaments. The rate of carbon filament formation is proportional to the particle size of Ni. Below a critical Ni particle size (d<2 nm), formation of carbon slowed down dramatically. Well dispersed Ni supported on ZrO_2 is thus a viable alternative to the noble metal based materials.

1. INTRODUCTION

Carbon dioxide reforming of methane to produce synthesis gas, i.e., a mixture of carbon monoxide and hydrogen ($CO_2+CH_4 \rightleftharpoons 2CO+2H_2$; $\Delta H^\circ_{298K} = 261.0$ kJ/mol) has attracted substantial interest [1-4]. The reaction route is well suited to produce CO rich syngas or very pure carbon monoxide for the synthesis of bulk chemicals such as acetic acid, dimethyl ether and alcohols *via* the oxoalcohols synthesis [5-7]. More significantly, for acetic acid manufacture carbon dioxide reforming is estimated to have economical advantages over other syngas production routes [6]. The reaction contains similar elementary reaction steps as in steam reforming ($H_2O+CH_4 \rightleftharpoons CO+3H_2$; $\Delta H^\circ_{298K} = +206.2$ kJ/mol) [8,9], but the absence of water and the higher C/H ratio in the reactant feed favors coke formation [10]. Minimization of coking rates is therefore one of the key aspects for designing a stable catalyst for the reaction. Coke forms readily *via* methane decomposition ($CH_4 \rightleftharpoons C+2H_2$; $\Delta H^\circ_{298K} = +74.9$ kJ/mol) and CO disproportionation ($2CO \rightleftharpoons C+CO_2$; $\Delta H^\circ_{298K} = -172.4$ kJ/mol) [11,12]. Options to reduce the coke build up are (i) the addition of water (coupling with steam reforming) [10], (ii) the addition of oxygen (coupling with partial oxidation) [7], or (iii) the use of catalysts which minimize the rate of coking [1].

We will report here on the last aspect, i.e., on the successful design of high temperature Pt and

Ni catalysts using ZrO_2 as a unique support that seems crucial to minimize coking under reaction conditions applied for CH_4/CO_2 reforming. For two successfully developed catalysts, (Pt and Ni on ZrO_2) the present contribution outlines the sequence of the elementary steps and the catalytic chemistry of the active metal and the support in order to explain catalysts activity and stability.

2. EXPERIMENTAL

2.1 Catalytic materials and reactants

Titania was obtained from Degussa (P25) and consisted of a mixture of anatase and rutile. ZrO_2 (RC100, Daichi Kigenso, Japan) contained only the monoclinic phase. γ-Al_2O_3 was obtained from Akzo-Nobel Chemicals (type 000-3AQ). The oxides were pressed into pellets and crushed to 0.3-0.6mm grains. These grains were then calcined at 1125K for 15 hours in a stream of dry flowing air (30 ml/min). The catalysts were typically prepared by impregnation of the calcined supports with aqueous 0.1 molar solutions of H_2PtCl_6 or $Ni(NO_3)_2$. Subsequently, the catalyst precursors were dried at 395K for 8 hours and calcined at 925K for 15 hours in flowing air (30 ml/min).

2.2 Catalytic experiments

Catalyst testing was performed in fixed bed (300 mg) continuous flow reactors (using a GC to analyze the products). The feed had a composition of CH_4/CO_2/He =1:1:2 and was passed over the catalyst with a space velocity of 28000 h^{-1} (GHSV). Prior to testing, the catalysts were typically reduced *in situ* with 5% H_2 in N_2 for one hour at 1125K in the case of Pt catalysts and at 875K in the case of Ni/ZrO_2. Coke formed on the catalyst was determined by combustion in oxygen and measuring the amount of carbon oxides generated [13,14].

2.3 Catalyst characterization

The reaction on the catalyst surface was followed by *in situ* i.r. spectroscopy using a Bruker IFS88 FTIR spectrometer for the characterisation of sorbed species and mass spectroscopy for the analysis of gas phase. The state of Pt was further investigated by *in situ* X-ray absorption spectroscopy (Daresbury, UK, beamline 9.1, transmission mode, Si(220) monochromator, Pt-L_{III} edge). Details of catalyst characterisation techniques are reported elsewhere [13,14].

3. RESULTS

3.1 Platina based catalysts

The characteristics of the supported Pt catalysts used in this study are compiled in Table 1. The activity of the catalysts during a typical time-on-stream experiment are shown in Fig 1. While Pt/ZrO_2 catalyst showed high stability (less than 5% loss in conversion during 180 hours time on stream), Pt/γ-Al_2O_3 lost all catalytic activity after 3 hours and Pt/TiO_2 deactivated gradually during 40 hours. The supports alone were catalytically inactive.

The amount of coke formed as a function of the number of turnovers is shown in Fig.2. The steeper slopes of these curves for Pt/γ-Al_2O_3 and Pt/TiO_2 indicate the higher selectivity of Pt/γ-Al_2O_3 and Pt/TiO_2 to form coke than Pt/ZrO_2. Hydrogen chemisorption capacity decreased markedly after some time on stream (see Table 2), but could be completely restored by oxidative treatment.

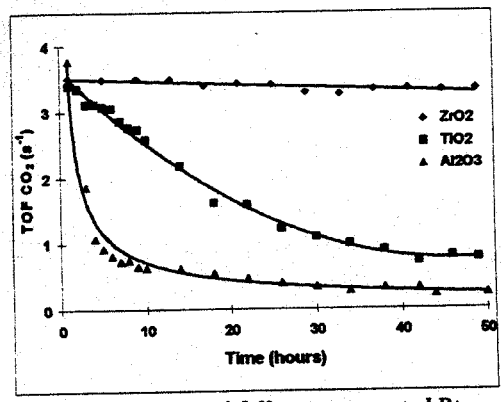

Figure 1 *Stability of different supported Pt catalysts for CO_2/CH_4 reforming at 875K*

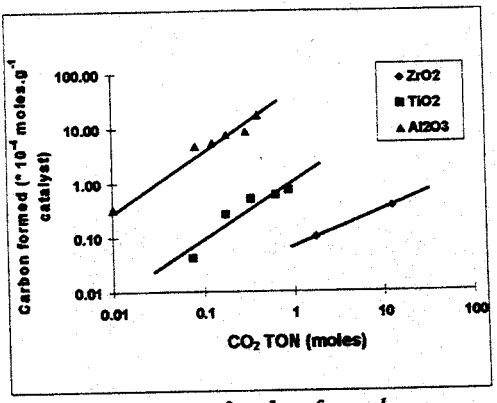

Figure 2 *Amounts of carbon formed as a function of the total amount of CO_2 converted for different Pt catalysts during CO_2/CH_4 reforming at 875K*

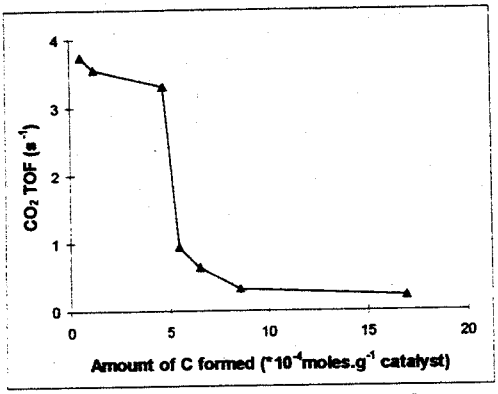

Figure 3 *Catalytic activity of $Pt/\gamma\text{-}Al_2O_3$ as function of the carbon deposited on the catalyst (875K)*

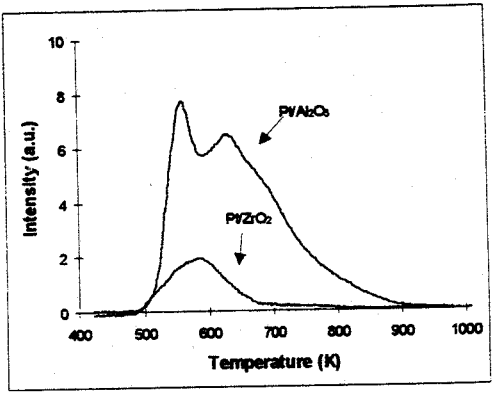

Figure 4 *Temperature programmed desorption of pyridine; pyridine adsorbed at 475K, heating rate 20K/min*

Table 1
Physicochemical properties of Pt catalysts investigated

Support	Metal loading (wt%)	BET Area ($m^2.g^{-1}$)	Pt dispersion* (%)
γ-Al_2O_3	0.5±0.2	112	35
TiO_2	0.5±0.2	5	25
ZrO_2	0.5±0.1	16	33

* catalysts were reduced at 1125K, Pt/H=1

While these observations link coking, blocking of active sites and catalytic activity, the results do not indicate to what extent the support contributes to coking and if such coke may physically block the access to the metal particles. To probe for the individual role of the support in coking,

Table 2
Hydrogen chemisorption capacity and catalytic activity

Catalyst	State	Pt dispersion (%)	[1]Rate of CO_2 convn. (10^{-5}. mol/g.s)
Pt/γ-Al_2O_3	fresh	35	3.4
	used[2]	8	0.3
	regenerated[3]	35	3.2
Pt/ZrO_2	fresh	33	3.2
	used[2]	9	3.1
	regenerated[3]	32	3.2

[1]at 875 K; [2]after testing at 875K for 25 hrs; [3]coke burned off in air at 675K

the weight of coke deposited after 25 hours on stream was compared for the supports and catalysts (see Table 3). It can be seen that the level of coking on Pt/γ-Al_2O_3 does not exceed that of the support alone. On the other two catalysts coke is reduced by the presence of Pt. In general, the extent of coking decreased in the order Al_2O_3>>TiO_2>ZrO_2 irrespective of the presence of Pt.

When the amount of coke formed as a function of time on stream is compared to the decrease in catalytic activity (see Fig. 3), two regimes of deactivation can be noticed for the strongly deactivating catalysts, i.e., a slow initial deactivation which is followed by a rapid loss of activity. This first phase is characteristic of a slow transformation of the reactive carbon into less reactive coke. The second phase is attributed to carbon formed on the support which accumulates there and rapidly covers the Pt particles when its amount reaches a critical value causing the sudden decay of catalytic activity.

This clearly indicates that the support is able to convert a fraction of methane but contributes primarily to coking. To investigate the role of acid sites in the conversion of methane to coke and hydrogen, the acid sites of the catalysts were characterized by sorption and temperature programmed desorption (t.p.d.) of pyridine. T.p.d. of pyridine (see Fig. 4) suggest a higher

concentration of stronger acid sites on $Pt/\gamma\text{-}Al_2O_3$ (presence of a second peak around 650 K) than on Pt/ZrO_2. I.r. spectra of adsorbed pyridine evidenced only Lewis acid sites on both catalysts.

3.2 Individual reaction steps on the Pt/ZrO_2

The question remaining now to be addressed is the role of reactants and catalyst phases in the network of reactions leading to CO, H_2 and carbon. For that purpose pulse reaction/titration experiments using the individual reactants mostly in sequence were applied.

Pulsing of methane at 875K over prereduced Pt/ZrO_2 yielded twice the number of moles of hydrogen in the gas phase indicating quantitative dissociation of methane. Fig. 5 shows the evolution of hydrogen as detected by mass spectrometry during pulsing of methane. As ZrO_2 was virtually inactive for methane dissociation, we conclude that Pt is the main catalytically active component. In contrast to ZrO_2, $\gamma\text{-}Al_2O_3$ was rather active in methane decomposition. This higher activity of $\gamma\text{-}Al_2O_3$ as compared to ZrO_2 parallels the higher concentration of Lewis acid sites on $Pt/\gamma\text{-}Al_2O_3$ and indicates that Lewis acid sites are affiliated with the catalytic activity of the support to dissociate methane.

Table 3
Coke deposition at 875K, after 25 hrs time on stream

Catalyst	Amount of coke (10^{-6} . mol/g)
$\gamma\text{-}Al_2O_3$	56
$Pt/\gamma\text{-}Al_2O_3$	59
TiO_2	14
Pt/TiO_2	6
ZrO_2	9
Pt/ZrO_2	1

Subsequent admission of oxygen in pulses indicated that carbon deposited by methane decomposition could be removed quantitatively by oxidation. The carbon remaining on the catalysts could also be quantitatively removed in the presence of Pt by CO_2. CO was the only reaction product.

In order to investigate whether CO_2 reacts in a concerted way with surface carbon or whether it dissociates first to CO and adsorbed oxygen and the adsorbed oxygen reacts, infrared spectroscopy, pulse reactor studies and XANES measurements were used. The *i.r.* spectrum of a prereduced (1hour at 675K in $5\%H_2/N_2$) Pt/ZrO_2 catalyst in contact with CO_2 at 775K is shown in Fig. 6. The spectrum shows the presence of linearly bound CO on Pt at 2053 cm^{-1} [15]. Additionally, bands of carbonate type species appeared in the region between 1375 and 1540 cm^{-1}. Over pure supports (in the absence of Pt) the CO band was not seen, but peaks in the carbonate region were observed.

The presence of CO on Pt (seen by the i.r. bands at 2053 cm^{-1}) indicates the dissociation of CO_2. This is further confirmed by the evolution of CO (detected by mass spectroscopy) during pulsing CO_2 over Pt/ZrO_2 and *in situ* XANES measurements. The XANES of the Pt $L\text{-}_{III}$ edge in the presence of reactant gases at 775K is shown in Fig. 7. The comparison of the Pt white lines in the presence of CO_2 and O_2 indicates that Pt is (partially) oxidized in the presence of CO_2 in all catalysts. This indicates rapid dissociation of CO_2 into CO and atomic oxygen as outlined above. The extent of the change of the Pt white line led us to conclude that not only the top most layer of the particles is involved, but also a considerable fraction of the bulk atoms takes part in the reaction. This is even more surprising as one notes how rapidly the white line changes between the oxidized state and a state characteristic of fully reduced Pt when one switches between CO_2 and oxygen containing atmosphere on the one hand and hydrogen and/or methane containing

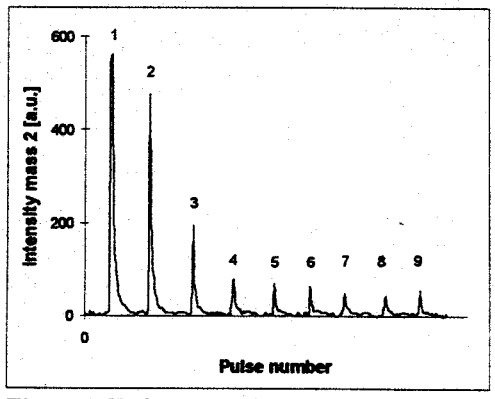

Figure 5 *Hydrogen evolution during methane pulsing over Pt/ZrO_2; 875K*

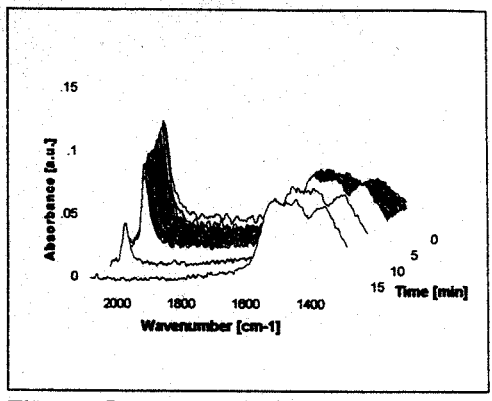

Figure 6 *I.r. spectra of Pt/ZrO_2 during contact with CO_2 at 775K*

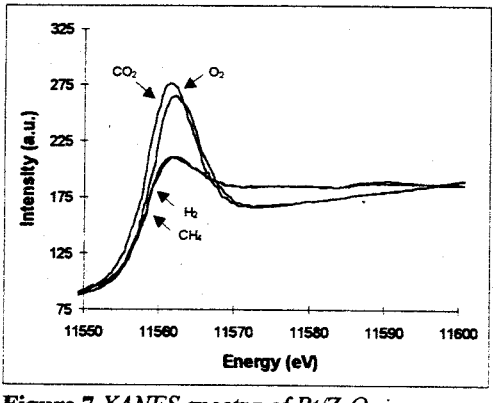

Figure 7 *XANES spectra of Pt/ZrO_2 in different gas atmospheres at 775K*

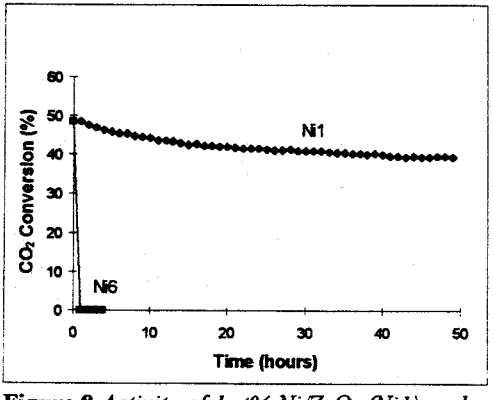

Figure 8 *Activity of 1wt% Ni/ZrO_2 (Ni1) and 6wt% Ni/ZrO_2 (Ni6) for CO_2/CH_4 reforming*

atmosphere on the other hand.

3.3 Ni/ZrO_2 catalysts

Characteristic physico-chemical properties of two typical catalysts are compiled in Table 4 [16]. Fig. 8 shows the activity of two Ni/ZrO_2 catalysts as a function of time. It can be seen that the catalyst containing the higher loading of Ni deactivated most rapidly, while the one with the low Ni loading was remarkably stable. The nature of coking in the case of Ni based catalysts is different from that of the noble metal based catalysts. Transmission electron microscopy (TEM) of the $6Ni/ZrO_2$ sample after one hour on stream (Fig. 9) shows the presence of filamentous carbon. The carbon filaments grew at the interface between Ni and ZrO_2. The presence of the Ni particle at the tip of the filament was checked by EDAX during the TEM measurement. However, filamentous carbon was not observed to be formed for $1Ni/ZrO_2$ after 50 hours time on stream.

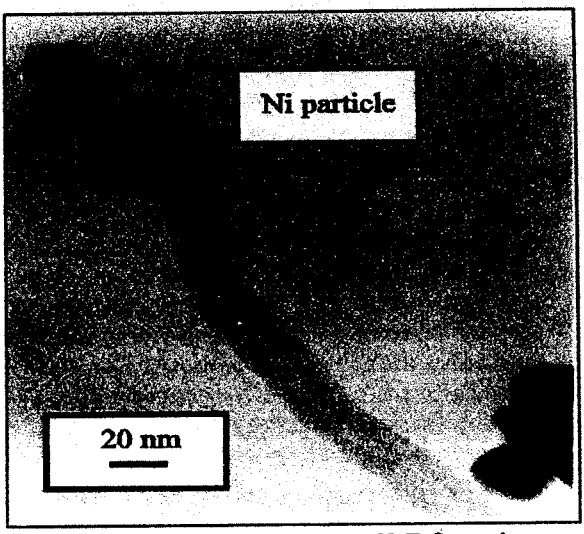

***Figure 9** Carbon filament formed on a Ni/ZrO_2 catalyst during CO_2/CH_4 reforming*

Table 4
Physicochemical characteristics Ni/ZrO_2 catalysts

Catalyst	BET area (m^2 /g)	Ni content (wt%)	Average Ni particle size (nm)
$1Ni/ZrO_2$	26	1.1	2
$6Ni/ZrO_2$	19	6.2	9

4. DISCUSSIONS

Steady state and non steady state kinetic measurements suggest that methane carbon dioxide reforming proceeds in sequential steps combining dissociation and surface reaction of methane and CO_2. During admission of pulses of methane on the supported Pt catalysts and on the oxide supports, methane decomposes into hydrogen and surface carbon. The amount of CH_4 converted per pulse decreases drastically after the third pulse (this corresponds to about 2-3 molecules of CH_4 converted per Pt atom) indicating that the reaction stops when Pt is covered with (reactive) carbon. CO_2 is also concluded to dissociate under reaction conditions generating CO and adsorbed

oxygen atoms. As nearly all of the carbon on Pt formed *via* methane decomposition can be oxidized in a concerted way by CO_2 or by the adsorbed oxygen produced from CO_2 (see Table 4) we conclude that the carbon on the surface is a reactive intermediate in the reforming reaction to yield CO. The overall reaction sequence can be summarized in the following elementary steps.

$$CH_4 + * \rightleftharpoons C* + 2H_2$$
$$CO_2 + 2* \rightleftharpoons CO* + O*$$
$$C* + O* \rightleftharpoons CO* + *$$
$$2CO* \rightleftharpoons 2CO + 2*$$
$$CH_4 + CO_2 \rightleftharpoons 2CO + 2H_2$$

Infrared spectroscopy and XAS measurements support this model of the reaction sequence. I.r. spectroscopy shows that CO is formed and adsorbed on Pt upon contacting the catalyst with CO_2 at 875K. *In situ* XAS measurements show that a large fraction of Pt (and not only the surface atoms) are oxidized by CO_2 at 775K indicating the presence of atomic oxygen on/in the Pt particles. Subsequent admission of methane completely reduced Pt in such a catalyst. Oxidation and reduction of Pt are rapid. It is important to emphasize that XAS measurements demonstrate that these processes are similar for all catalysts investigated indicating that the support does not induce a particular surface chemistry on Pt. This is in accordance with the similar intrinsic activity of Pt sites (TOF, in Fig.1) of all catalysts.

The carbonate species seen on the supports irrespective of the presence of Pt do not seem to play a key role in the catalytic cycle.

Let us now use the sequence of elementary steps to explain the activity loss for some of the catalysts. The combination of hydrogen chemisorption and catalytic measurements indicate that blocking of Pt by coke rather than sintering causes the severe deactivation observed in the case of $Pt/\gamma\text{-}Al_2O_3$. The loss in hydrogen chemisorption capacity of the catalysts after use (Table 2) is attributed mainly to carbon formed by methane decomposition on Pt and impeding further access. Since this coke on Pt is a reactive intermediate, Pt/ZrO_2 continues to maintain its stable activity with time on stream.

Coke formation on these catalysts occurs mainly *via* methane decomposition. Deactivation as a function of coke content (see Fig. 3 for $Pt/\gamma\text{-}Al_2O_3$) seems to involve two processes, i.e., a slow initial one caused by coke formed from methane on Pt that is non reactive towards CO_2 (see Table 3). In parallel, carbon also accumulates on the support and given the ratio between the support surface and metal surface area at a certain level begins to physically block Pt deactivating the catalyst rapidly. The coke deposited on the support very close to the Pt- support interface could be playing an important role in this process.

Using the t.p.d. and i.r. spectra of adsorbed pyridine we conclude that high concentrations of Lewis acid sites (e.g., present on $\gamma\text{-}Al_2O_3$) are responsible for high rates of coking. Such coke on the support is difficult to be removed by CO_2 as pure supports showed no catalytic activity. Therefore, coke formed on the support causes deactivation when it covers Pt. This corresponds to the rapid decay of activity seen, for example, for $Pt/\gamma\text{-}Al_2O_3$ (Fig.3). The small continuous loss in activity (for all catalysts) may be due to part of the coke formed from methane on Pt undergoing aging which makes it non reactive. Thus, we conclude that it is the uniquely low concentration of weak Lewis acid sites on the ZrO_2 support that seems to be indispensable for minimizing coking in Pt/ZrO_2. Addition of Pt could be reducing the number of Lewis sites on ZrO_2

further and explains why Pt/ZrO_2 forms even less coke than ZrO_2 (Table 3).

In contrast to the Pt catalysts discussed above, Ni based catalysts (i.e., also when supported on ZrO_2) usually form coke at such a rapid rate that most fixed bed reactors are completely blocked after a few minutes time on stream (see Fig. 8) [16]. The coke formed with the Ni catalysts is filamentous. The Ni particle remaining at the tip of the filament hardly deactivates as the coke formed on its surface seems to be transported through the metal particle into the carbon fibre, but the drastic increase in volume causes reactor plugging and prevents use of the still active catalyst (see Fig. 8). The TEM photographs indicate that the carbon filaments have similar diameters to those of the Ni particles.

As the metal particle size decreases the filament diameter should also decrease. It has been shown that the surface energy of thinner filaments is larger and hence the filaments are less stable (11, 17-18). Also the proportion of the Ni(111) planes, which readily cause carbon formation, is lower in smaller Ni particles (19). Therefore, even though the reasons are diverse, in practice the carbon filament formation ceases with catalysts containing smaller Ni particles. Consequently, well dispersed Ni catalysts prepared by deposition precipitation of Ni (average metal particle size below 2-3 nm) were stable for 50 hours on stream and exhibited no filamentous coke [16].

5. CONCLUSIONS

Methane reforming with carbon dioxide proceeds in a complex sequence of reaction steps involving the dissociative adsorption/reaction of methane and CO_2 at metal sites. Hydrogen is generated during methane dissociation. In the second set of reactions CO_2 dissociates into CO and adsorbed oxygen. The reaction between the surface bound carbon (from methane dissociation) and the adsorbed oxygen (from CO_2 dissociation) yields carbon monoxide. A stable catalyst can only be achieved if the two sets of reactions are balanced.

Two ways to design such a stable catalysts are described. The support and the active metal play an important role in ensuring catalyst stability. For a noble metal such as Pt, which itself has a low tendency to form coke [1], the minimization of the concentration of acid sites on the support is most critical. ZrO_2 is unique in that respect as it combines strong anchoring of the Pt metal particle (important for high temperature operation) and very low concentrations of (Lewis) acid sites (important for minimizing carbon formation on the support). Excellent results were obtained with a $0.5wt\%Pt/ZrO_2$ catalyst which proved to be well suited for upscaling [20].

For non-noble metal catalysts, such as oxide supported Ni, also the metal function has to be adapted to minimize coke formation. This results from the fact that the rate of methane decomposition over Ni catalysts is enhanced relative to CO_2 dissociation leading to a significantly higher concentration of carbon at the Ni particle. This triggers transport of the carbon through the Ni particle and formation of (hollow) carbon filaments carrying the metal particle at the top. It was found that reducing the size of the Ni particles slows down the overall rate of formation of the carbon filament. Thus, preparing a Ni/ZrO_2 catalyst with a particle size below 2nm prevented the generation of filamentous coke and allowed stable operation for prolonged periods.

Acknowledgments

We gratefully acknowledge the support for this work from the JOULE II Programme (Energy from fossil fuels: Hydrocarbons, contract no. JOU2-CT92-0073) and Human Capital and Mobility Programme (contract no. ERB4001GT941163) of the European Union. The authors are indebted to M. Englisch and A. Jentys for valuable discussions on XANES of Pt/ZrO_2.

6. REFERENCES

1. A.T. Ashcroft, A.K. Cheetham, M.L.H. Green and P.D.F. Vernon, Nature, 225 (1991) 352.
2. J.T. Richardson and S.A. Paripatyadar, Appl. Catal., 61 (1990) 293.
3. K. Seshan and J.A. Lercher, in J. Paul and C. Pradier, (Eds.) "Carbon dioxide: Environmental issues", The Royal Soc. Chem., Cambridge, 1994, p16.
4. A. Bhattacharya and V.W. Chang, Int. Conf. on Catalyst Deactivation, Oostende, Oct., 1994, Stud. Surf. Sci Catal. 88 (1994) 207.
5. G. Kurz and S. Teuner, Erdol. Kohle, 43(5) (1990) 171.
6. P.F. van den Oosterkamp, Q. Chen, J.A.S. Overwater, J.R.H. Ross and A.N.J. van Keulen, Meeting of "Large Chemical Plants", Antwerp, Belgium, Oct., 1995.
7. Gas Process Handbook '92, Hydocarbon Processing, 90, (1992).
8. I.M. Bodrov, L.O. Apel'baum, Kinet. Katal. 8 (1967) 379.
9. J. R. Rostrup Nielsen, J. Catal., 144, (1993) 38.
10. N.R.Udengaard, J.H. Bak Hansen, D.C. Hanson, J.A. Stal, Oil Gas J., 90 (1992) 62.
11. J.R. Rostrup-Nielsen, J.Catal., 27 (1972) 343.
12. R.T.K. Baker, M.A. Barber, P.S. Harris, F.S. Feates and R.J. Waite, J.Catal., 26 (1972) 51.
13. K. Seshan, H.W. ten Barge, W. Hally, A.N.J. van Keulen, J.R.H. Ross, Stud. Surf. Sci. Catal. 81 (1994) 285.
14. J.H. Bitter, W. Hally, K. Seshan, J.G. van Ommen and J.A. Lercher, Catal. Today, accepted for publication (1995).
15. L.H. Little, Infrared Spectra of Adsorbed Species,, Academic Press, New York, 1966, p 54.
16. W. Hally, H.J. Bitter, K. Seshan, J.R.H. Ross, and J.A. Lercher, Int. Conf. on Catalyst Deactivation, Oostende, Oct., 1994, Stud. Surf. Sci. Catal. 88 (1994) 167.
17. I. Alstrup, J. Catal., 109 (1988) 241.
18. P.K. de Boks, A.J.H.M. Kock, E. Boelleerd, W. Klop, J.W. Geus, J. Catal., 96 (1985) 454.
19. C.H. Bartholomew, Cata. Rev. Sc. & Engg., 24, 67 (1982)
20. K. Seshan, P.D.L. Mercera, E. Xue, J.R.H. Ross, German Patent, P43 13 673.7 (1993), US Patent Appl. PCT/DE94/00513 dated (1994)